ISSN 1392–1320 MATERIALS SCIENCE (MEDŽIAGOTYRA). Vol. 22, No. 3. 2016

The Microstructure and Compressive Properties of Aluminum Alloy (A356) Foams with Different Al-Ti-B Additions

Zan ZHANG [1], Jing WANG [1], Xingchuan XIA [1 *], Weimin ZHAO [1, 2], Bo LIAO [1], Boyoung HUR [3]

[1] *School of Materials Science and Engineering, Hebei University of Technology, Dingzigu, Hongqiao district, Tianjin 300130, China*
[2] *Key Lab for Micro- and Nano-Scale Boron Nitride Materials in Hebei Province*
[3] *School of Nano'Advanced Materials Science and Engineering, Gyeongsang National University of South Korea, Republic of Korea*

crossref http://dx.doi.org/10.5755/j01.ms.22.3.8559

Received 26 October 2014; accepted 31 March 2015

Closed-cell aluminum alloy (A356) foams with different percentages of Al-Ti-B are prepared by melt foaming method, using Ca and TiH_2 as thickening agent and foaming agent, respectively. SEM and Quasi-static compression tests are performed to investigate the effect of Al-Ti-B on the microstructure and compressive properties of aluminum alloy (A356) foams. The results show that foams with Al-Ti-B percentage of 0.3 wt.% possess good combinations of micro hardness, yield strength, plateau strength, densification strain and energy absorption capacity under the present conditions. The reasons are mainly due to the foams with Al-Ti-B percentage of 0.3 wt.% possess optimal eutectic Si morphology (with eutectic Si existing in the forms of particles or short fiber).
Keywords: aluminum foam, melt foaming method, Al-Ti-B, microstructure, compressive property.

1. INTRODUCTION

Metal foams are a relatively new class of materials showing unique combination properties that cannot be obtained by any dense metals, even for foamed polymeric or ceramic materials [1 – 3]. According to the connectivity of the pores, metal foams can be divided into open-cell or closed-cell. Open-cell foams are mainly used as functional materials, such as heat exchangers, catalyst carrier because of their good permeability for fluids and large surface area. Closed-cell foams are mainly used in the load bearing and energy absorbing fields due to their higher yield strength and plateau stress [2, 3]. Among all of the metallic metal foams, closed-cell aluminum foams have been utilized more extensively than other foams in such services as energy absorber, light-weight structures, in-door sound absorbers, automobile roofs and crash-energy absorption elements of space vehicles [4]. In addition, as Si-containing aluminum alloys possess excellent castability, good corrosion resistance and weldability, in the last two decades, more and more researchers have been focusing on the manufacturing process and characterizing the properties of Si-containing aluminum alloy foams [1, 5 – 6].

Yang and Nakae [7] investigated the effect of foaming agent content and foaming temperature on the macrostructure of aluminum alloy foam (A356) and the results showed that a properly controlled holding temperature of the melt and the titanium hydride content were good for the acquirement of foamed aluminum. Fabrizio et al. [8] produced aluminum alloy (AlSi7Mg0.3) foams with a relative density of ~35 % by replication of salt precursors and reported that the distribution of grain size is homogeneous in the foams. Malekjafarian and Sadrnezhaad [9] studied the effect of density (porosity) on the mechanical properties of composite foams (with A356/SiC composite as matrix). Meanwhile, Ravi Kumar, et al. [10] investigated the effect of SiC content on the foaming behavior and mechanical properties of A356/SiC composite foams and the results showed that the presence of SiC could lead to good foaming behaviors. While, SiC content had an unconspicuous effect on the compressive plateau strength of the foams. Schüler, et al. [11] studied the deformation behavior and mechanical properties of aluminum alloy (A356) foams under quasi-static and dynamic loading conditions.

Mechanical properties of Si-containing aluminum foams are generally dependent on the strength of basic materials, relative density and morphology of the foams [12]. In addition, the strength of the basic materials is mainly due to the microstructure morphologies of the cell walls. Some of the critical microstructure characteristics are grain size and the morphology of eutectic silicon [13]. Meanwhile Al-Ti-B ternary master alloys, particularly for Al-5Ti-1B, have been widely used as aluminum alloys grain refiners to improve their mechanical properties [14 – 19]. Though the solidifications of aluminum alloy (A356) and aluminum alloy (A356) foam are volume solidification, the cooling rates between the alloy and foam are quite different [20], which may result in different strengthen mechanisms of Al-Ti-B in aluminum alloy and aluminum alloy foams. As described above, though researchers have focused on the production and mechanical properties of aluminum alloy (A356) foams, the effect of the microstructure and micro-morphology on the

* Corresponding author. Tel.: +86 22 60202414; fax: +86 22 60204477.
E-mail address: *xc_xia@hebut.edu.cn* (X. Xia)

compressive properties of these foams are seldom involved in and further research is needed. Therefore, the aim of this study is to investigate the effect of Al-Ti-B ternary master alloys on the variation of micro- morphology of A356 aluminum alloy foam, and more importantly to evaluate the effect of Al-Ti-B on the compressive properties of A356 aluminum alloy foams.

2. MATERIALS AND EXPERIMENTS

Melt foaming method is applied to fabricate A356 aluminum alloy foams with different percentages of Al-Ti-B. In the present experiment, commercial A356 aluminum alloy (Al-7Si-0.4Mg) is used as base material. Commercially pure Al powders ($\geq$ 99.5 wt.%) and TiH_2 powders (300 ± 20 mesh) are used as thickening agent and foaming agent, respectively. Al-Ti-B master alloy (Commercially pure, with 5 wt.% Ti, 1 wt.% B) is used to modify the morphology. The preparation procedures mainly include the following steps: (1) melting certain quality of raw material (~1 kg) in a low carbon steel crucible to a fixed temperature, boron nitride (nano-scale, Key Lab for Micro- and Nano-Scale Boron Nitride Materials in Hebei Province) is applied to prevent the diffusion of Fe into the melt; (2) adding different contents of (0 %, 0.2 %, 0.3 %, 0.4 %, 0.6 % and 0.8 wt.%, hereinafter % refers to wt.%) Al-Ti-B to the melt; (3) adding certain amount of Al powders (2%) to the melt accompanied by stirring, with the stirring speed of 800 rpm for 10 min. The impellor is driven by an electromotor and the stirring speed is controllable [21]; (4) adding certain quantity of TiH_2 (1.2 %) to the melt accompanied by stirring, with the stirring speed of 1200 rpm for 30 s and then holding the slurry for 2 min; (5) cooling the crucible in the air after it is foamed (A356 aluminum alloy foam with Al-Ti-B contents of 0 %, 0.2 %, 0.3 %, 0.4 %, 0.6 % and 0.8 %, henceforth referred as ATB0, ATB0.2, ATB0.3, ATB0.4, ATB0.6 and ATB0.8, respectively). During the whole procedures except for the last step the temperature of the melt is controlled at 933 ± 5 K. Specimens for microstructure observation are machined by electro-discharging machining [22]. Representative metallographic preparation processes are applied to prepare specimens for metallographic characterization. Specimens are finally ground using 2000 grit emery paper, polished using 0.25 μm diamond paste and then etched using 2 vol.% hydrofluoric acid alcohol. Microstructures of the aluminum alloy foams are examined by a Hitachi S4800 scanning electron microscope (SEM) equipped with energy dispersive X-ray spectrometer (EDX), and the average grain size is calculated by the linear intercept method. The phase composition is examined by X-ray diffraction (XRD) (SmartLab, Rigaku) with CuKa radiation.

Specimens for compression tests are machined into the size of 25 × 25 × 25 mm^3 by electro-discharging machine to avoid size effect. The porosity of the foam is deduced from mass and volume. Analytical balance (with the precision of 0.0001 g) and caliper are used to measure the weights and accurate dimensions, respectively. Uniaxial compression tests are performed by using SUNS Electron Universal Material Testing Machine, with a maximum load of 300 KN. All tests are performed under displacement control, with a displacement rate of 1.5 mm/min (with the initial strain rate of 0.001/s) at room temperature. In this paper, the first peak stress of the deformation curve is defined as yield strength. Vaseline is used to minimize the friction between sample and plates. Load and displacement are recorded automatically by a computer, engineering stress σ is defined as the load (KN) on specimen divided by specimen cross area; engineering strain ε is defined as the displacement (mm) of specimen divided by specimen height (mm). Extrapolation method is used to determine the densification strain [23]. Cell wall micro hardness is tested on a SHIMADZU micro-hardness tester with Vickers pyramid and load of 10 g. At least 10 points are selected randomly and the average data are employed.

3. RESULTS AND DISCUSSION

3.1. Specimens of Al alloy (A356) foams

Fig. 1 shows the typical morphology of a specimen used for compression test. It can be seen that the cell structure is homogeneous. The pore sizes and porosities of the foam produced in the present experiment are mainly distributed in 1 – 3 mm and 75 – 85 %, respectively. It should be noted that ATB0.6 and ATB0.8 fracture in the middle when being took out of the crucible, indicating that the foams are brittle and not easy to keep their integral structures.

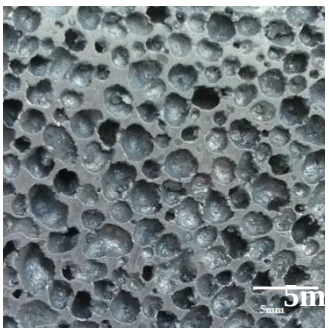

Fig. 1. Optical cross section of compression specimen with Al-Ti-B percentage of 0.2%

3.2. Micro-morphology of Al alloy (A356) foams

XRD analysis (as shown in Fig. 2) on ATB0.3 is applied to investigate the evaluation of the phases in the foams. It shows that α-Al, Si, TiB_2, $TiSi_2$, SiTi, Al_5Ti_2 and Al_3Ti phases exist in the foam. In order to understand the influence of Al-Ti-B on the micro-morphology of the foams, SEM and EDS tests (as shown in Fig. 3) are applied on the cell walls. It can be seen that foam cell walls are mainly composed of α-Al and eutectic Si. On the whole, Al-Ti-B has little influence on the grain size of α-Al. While the grain size is influenced by super-cooling degree and the number of heterogeneous nucleation particles [24, 25]. The cooling rate of foams is slow because of the existence of gas, larger super-cooling degree is needed to nucleate. In the case of A356 Al alloys, where Si content is 7 wt.%, the refining efficiency of commercial Al-Ti-B master alloys is relatively poor. This is due to the interaction of Ti with Si to form titanium silicides (as shown in Fig. 2) which depletes the melt of Ti preventing grain refinement of the alloy. This phenomenon has been

the subject of different studies and it is known as poisoning effect [26 – 29].

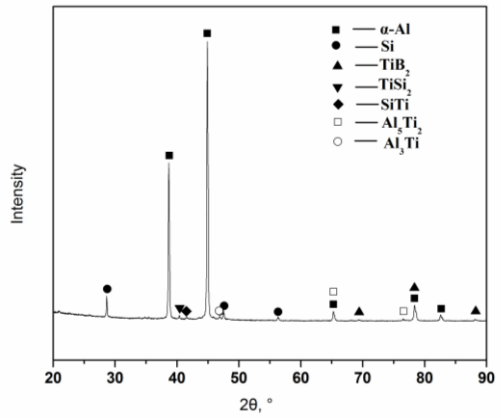

Fig. 2. XRD pattern of ATB0.3

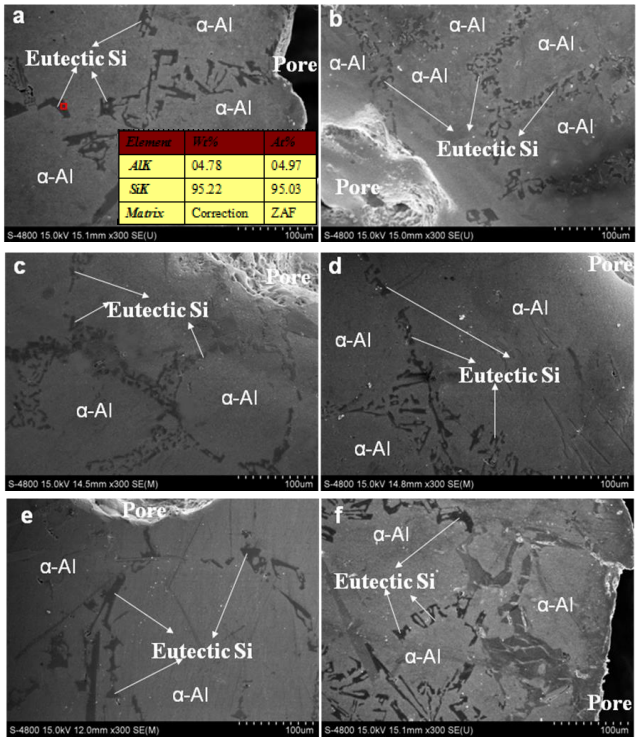

Fig. 3. SEM and EDS results of Al alloy foams with Al-Ti-B contents of a – 0 %; b – 0.2 %; c – 0.3 %; d – 0.4 %; e – 0.6 %; f – 0.8 %

In addition, liquid of aluminum alloy with Al-Ti-B should be used up in a certain time. While in this study Al-Ti-B is kept in aluminum alloy melt in the processes of thickening, foaming, holding and cooling, which accelerates fading of Al-Ti-B, hence decreasing the grain refine efficiency. Not only heterogeneous nucleation but also growth restriction impact on effective refinement [30]. The grains may grow up again as the foams with low thermal conductivity solidify slowly. Therefore, α-Al grain size is not refined apparently. It is clear that the distribution of the eutectic Si is along with the grain boundaries. However, Al-Ti-B has a significant impact on the morphology of eutectic Si. For ATB0 the eutectic Si is coarse (as shown in Fig. 3 a). For ATB0.2 part of the eutectic Si changes into small pieces (as shown in Fig. 3 b). For ATB0.3 most of the eutectic Si exists in the forms of fine blocks or short fibers (as observed in Fig. 3 c). However, further increment of Al-Ti-B causes the coarsening of eutectic Si that becomes blocky again (as shown in Fig. 3 d, e and f). This, means that excessive Al-Ti-B could not refine the morphology of eutectic Si.

3.3. Mechanical properties

Fig. 4 shows the variation tendency of cell walls' micro-hardness. It should be noted that the micro-hardness tests are performed on the cell wall matrix rather than on the cell wall grain boundary. It is clear that Al-Ti-B additions have an effect on the cell walls' micro-hardness. In summary, the micro-hardness of foams increases firstly and then decreases with the increase of Al-Ti-B content. The values (HV) of ATB0, ATB0.2, ATB0.3, ATB0.4, ATB0.6 and ATB0.8 are about 45.1, 45.76, 48.68, 46.71, 40.23 and 36.84, respectively. Compared with ATB0, the micro-hardness of ATB0.2, ATB0.3 and ATB0.4 increase slightly and ATB0.3 possesses the highest micro-hardness under the present conditions. However, for ATB0.6 and ATB0.8 the values drop significantly compared to ATB0.

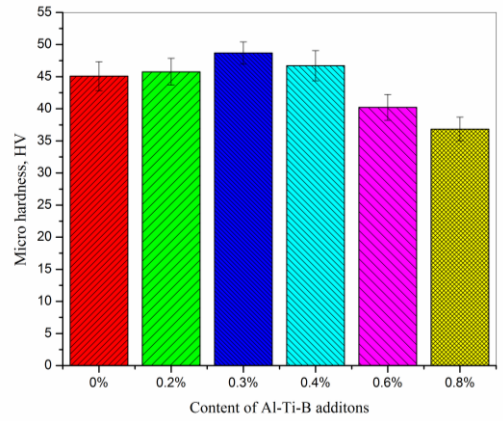

Fig. 4. Micro hardness variation tendency of the specimens with different contents of Al-Ti-B

Quasi-static engineering stress (σ)-strain (ε) compression curves of aluminum alloy foams with uniform porosity (~80 %) but different Al-Ti-B contents (0 %, 0.2 %, 0.3 %, 0.4 %, 0.6 % and 0.8 %) are shown in Fig. 5 a. The curves follow typical behavior of cellular foams with three deformation stages: (a) an initial elastic-plastic deformation stage, where partially reversible cell walls bending occurs [31, 32]; (b) an extended plateau stage, where cell walls buckle, yield and quantity fracture and (c) a rapidly increasing stress, where the cell walls become compacted together and the material attains bulk-like properties [32]. It can be seen that the additions of Al-Ti-B have an important effect on the stress-strain curves of Al alloy foams. Meanwhile, it should also be noted that the yield strength of the foams increased first and then decrease with the increase of Al-Ti-B contents: the yield strength of ATB0, ATB0.2, ATB0.3, ATB0.4, ATB0.6 and ATB0.8 are about 1.5, 2.1, 3.3, 1.6, 0.9 and 0.7 MPa, respectively. It is obvious that the yield strength of ATB0.3 is more than twice of ATB0. However, the yield strength of ATB0.4 decline sharply (as shown in Fig. 5 b) to 1.6 MPa. For ATB0.6 and ATB0.8, the values are about half of ATB0. All this means that the Al-Ti-B content should be controlled to get optimal yield strength. In addition, the strain of yield strength for ATB0.3 is about 0.05, while the

values for ATB0, ATB0.2, ATB0.4, ATB0.6 and ATB0.8 are approximately 0.025. In the extended plateau stage, the mean plateau stresses (defined as the average value of the stress with the strain between 0.10 and 0.45) increase first and then decrease with Al-Ti-B content increasing (as shown in Fig. 5 b). The mean plateau stresses of ATB0, ATB0.2, ATB0.3, ATB0.4, ATB0.6 and ATB0.8 are about 1.77, 2.60, 2.91, 2.26, 1.53 and 1.33 MPa, respectively. It is noted that ATB0.3 possesses the highest mean plateau stress under the present conditions. While, the values for ATB0.6 and ATB0.8 are lower than ATB0. Fig. 5 b shows the variation tendency of densification strains of aluminum alloy foams with different Al-Ti-B additions. It can be seen that Al-Ti-B additions have a significant influence on the densification strain. The densification strain for ATB0 is about 0.57 and the value increases to 0.65 for ATB0.3 and then decreases rapidly.

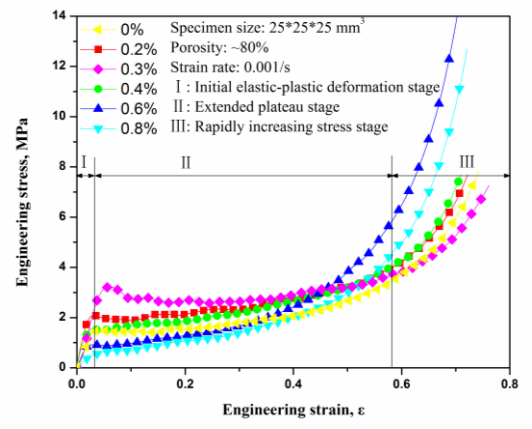

a

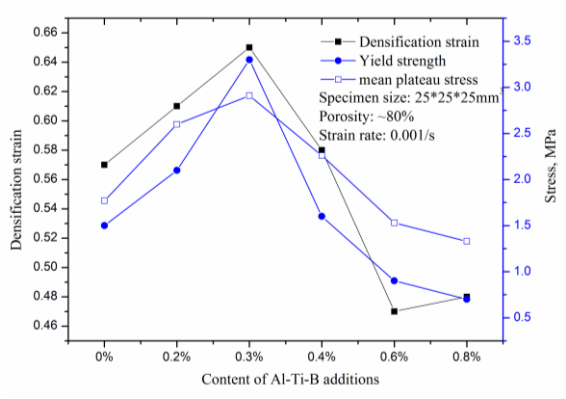

b

Fig. 5. a – quasi-static compressive engineering stress (σ)-engineering strain (ε) curves of aluminum alloy foams with different contents of Al-Ti-B; b – variation tendencies of densification strain, mean plateau stress and yield strength

Up to now, metal foams are mainly applied in energy absorption fields. The energy absorption capacity of material can be evaluated by integrating the area under the stress-strain curve, which can be denoted as Eq. 1:

$$W = \int_0^{\varepsilon} \sigma d\varepsilon \quad , \tag{1}$$

where W is the energy absorbed capacity of foams, σ is the stress where the strain is ε [33]. As shown in Fig. 6, in all cases energy absorption capacities increase with strain increasing. In addition, Al-Ti-B has a significant influence on the energy absorption capacity. It is observed that the curves for ATB0.2, ATB0.3 and ATB0.4 approximate to linearity, which is similar to curve of ATB0. While for the ATB0.6 and ATB0.8, the curves are obviously different from the curve of ATB0. In addition, during the compression test it is important to evaluate the energy absorbed before the foam is compacted, because if the foam is compacted the buffering effect will be decreased seriously [34]. Here available energy absorption capacity (AEAC, defined as the energy absorbed until the densification strain during the compression test [34]) is used to assess the energy absorption capacity of foams under the present conditions. It can be seen that the AEAC for ATB0, ATB0.2, ATB0.3, ATB0.4, ATB0.6 and ATB0.8 are about 1.06, 1.58, 1.90, 1.34, 0.74 and 0.62 MJ/m^3, respectively. It should also be noted that ATB0.3 possess the highest AEAC value and excessive Al-Ti-B additions will deteriorate the AEAC value. It indicates that appropriate amount of Al-Ti-B additions can intensify the AEAC.

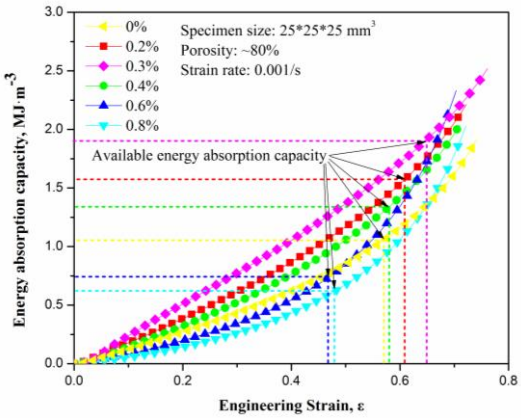

Fig. 6. Energy absorption capacities of Al alloy foams with different contents of Al-Ti-B

As described above ATB0.3 possesses good combination of micro-hardness, yield strength, plateau stress, densification strain and energy absorption capacity under the present conditions. Mechanical properties of metal foams are generally depended on the strength of basic materials, relative density, macro- and micro-morphology of the foams [12, 35]. In this paper, the basic material and relative density of the foams are almost identical, meaning macro-morphologies of the foams are similar too. Thus, the mechanical properties should mainly depend on micro-morphologies of the foams. As described above, the grain sizes of the foams change little with the addition of Al-Ti-B. Meanwhile, it has been confirmed that the most important micro-morphology in A356 aluminum alloys is the form of eutectic Si, which has a determinative effect on the alloys mechanical properties [13]. For ATB0.3 most of eutectic Si exist in the forms of fine particles or short fibers (as observed in Fig. 3 c). This indicates that refinement of eutectic Si can strengthen mechanical properties of aluminum (A356) foam. In addition, precipitated phases in the foams act as obstacles to the movement of dislocations during the loading of the foams [36]. It is likely for dislocation line to loop around the particles by Orowan looping rather than to cut through them. According to Orowan strengthen mechanism, dislocation loops provide more resistance to the movement of subsequent dislocations and thus increase the strength of

the composites [37, 38]. Also, append dislocations are created due to the difference of the coefficient of thermal expansion between the matrix and TiB_2 particles, thus these dislocations make the plastic deformation more difficult. It is interesting to note that the aluminum alloy foams with excess Al-Ti-B do not behave the highest micro-hardness and compressive properties. It is considered that the increasing Al-Ti-B additions results in too many inclusions, some of which with big sizes and agglomerated distribution may act as crack sources during the compressive deformation and hinder further improvement of the mechanical properties. All of these reasons lead to the appropriate compressive properties of foams with Al-Ti-B content of 0.3 %.

4. CONCLUSIONS

In the study, the microstructure and compressive properties of aluminum alloy foams with different contents of Al-Ti-B are investigated. The results are summarized as follows:

Aluminum alloy (A356) foams with Al-Ti-B content of 0.3 % possess good combinations of the micro-hardness, yield strength, plateau strength, densification strain and energy absorption capacity under the present conditions. In addition, Al-Ti-B has important effect on the morphology of eutectic Si, the eutectic Si will change into particles or short fibers with Al-Ti-B addition of 0.3 %, leading to optimal mechanical properties under present conditions. In the case of higher Al-Ti-B content the eutectic Si will become coarser again, and the increasing Al-Ti-B additions results in too many inclusions, which hinder further improvement of the mechanical properties.

Acknowledgements

The present authors wish to thank the financial support provided by Hebei Province School Cooperation Fund Projects, National Natural Science Foundation of China (No.51501053), "863" project of China (NO.2013AA031002), Major Project of China (2013ZX04004027), by Program for Changjiang Scholars and Innovative Research Team in University (No.IRT13060), Science and Technology Project of Hebei Province (13211008D).

REFERENCES

1. **Lefebvre, L.-P., Banhart, J., Dunand, D.** Porous Metals and Metallic Foams: Current Status and Recent Developments *Advanced Engineering Materials* 10 2008: pp. 775 – 787. http://dx.doi.org/10.1002/adem.200800241
2. **Banhart, J.** Manufacture, Characterisation and Application of Cellular Metals and Metal Foams *Progress in Materials Science* 46 2001: pp. 559 – 632.
3. **Ashby, M.-F., Evans, A., Fleck, N.-A., Gibson, L.-J., Hutchinson, J.-W., Wadley, H.-N.-G.** Metal Foams: A Design Guide, Butterworth Heinemann, Boston, MA, 2000.
4. **Banhart, J., Ashby, M.-F., Fleck, N.** Cellular Metal and Metal Foaming Technology. Germany, Verlag MIT; 2001.
5. **Orbulov, I.-N.** Metal Matrix Syntactic Foams Produced by Pressure Infiltration—The Effect of Infiltration Parameters *Materials Science & Engineering A* 583 2013: pp. 11 – 19.
6. **Orbulov, I.-N., Ginsztler, J.** Compressive Characteristics of Metal Matrix Syntactic Foams *Composites: Part A* 43 2012: pp. 553 – 561. http://dx.doi.org/10.1016/j.compositesa.2012.01.008
7. **Yang, C.-C., Nakae, H.** Foaming Characteristics Control During Production of Aluminum Alloy Foam *Journal of Alloys and Compounds* 313 2000: pp. 188 – 191.
8. **Quadrini, F., Alberto, B., Ludovica, R., Loredana, S.** Replication Casting of Open-cell AlSi7Mg0.3 Foams *Materials Letters* 65 2011: pp. 2558 – 2561. http://dx.doi.org/10.1016/j.matlet.2011.05.057
9. **Malekjafarian, M., Sadrnezhaad, S.-K.** Closed-cell Al Alloy Composite Foams: Production and Characterization *Materials and Design* 42 2012: pp. 8 – 12.
10. **Kumar, N.-V.-R., Rao, N.-R., Gokhale, A.-A.** Effect of SiC Particle Content on Foaming and Mechanical Properties of Remelted and Diluted A356/SiC Composite *Materials Science & Engineering A* 598 2014: pp. 343 – 349. http://dx.doi.org/10.1016/j.msea.2014.01.050
11. **Paul, S., Sebastian, F.-F., Andreas, B.-P., Claudia, F.** Deformation and Failure Behaviour of Open Cell Al Foams under Quasistatic and Impact Loading *Materials Science & Engineering A* 587 2013: pp. 250 – 261.
12. **Gibson, L.-J., Ashby, M.-F.** Cellular Solids: Structure and Properties, 2nd ed, Pergamon Press, Oxford, 1997. http://dx.doi.org/10.1017/CBO9781139878326
13. **Mohanty, P.-S., Gruzleski, J.-E.** Grain Refinement Mechanisms of Hypoeutectic Al-Si Alloys *Acta Materialia* 44 (9) 1996: pp. 3749 – 3760. http://dx.doi.org/10.1016/1359-6454(96)00021-3
14. **Han, Y.-F., Li, K., Wang, J., Shu, D., Sun, B.-D.** Influence of High-intensity Ultrasound on Grain Refining Performance of Al–5Ti–1B Master Alloy on Aluminum *Materials Science & Engineering A* 405 2005: pp. 306 – 312.
15. **Easton, M.-A., Stjohn, D.-H.** A Model of Grain Refinement Incorporating Alloy Constitution and Potency of Heterogeneous Nucleant Particles *Acta Materialia* 49 2001: pp. 1867 – 1878.
16. **Schaffer, P.-L., Dahle, A.-K.** Settling Behaviour of Different Grain Refiners in Aluminum *Materials Science & Engineering A* 413 – 414 2005: pp. 373 – 378.
17. **Birol, Y.** Production of Al–Ti–B Grain Refining Master Alloys from B_2O_3 and K_2TiF_6 *Journal of Alloys Compounds* 443 2007: pp. 94 – 98. http://dx.doi.org/10.1016/j.jallcom.2006.10.009
18. **Birol, Y.** Production of Al–Ti–B Grain Refining Master Alloys from $Na_2B_4O_7$ and K_2TiF_6 *Journal of Alloys Compounds* 458 2008: pp. 271 – 276. http://dx.doi.org/10.1016/j.jallcom.2007.04.036
19. **Li, P.-T., Ma, X.-G., Li, Y.-G., Nie, J.-F., Liu, X.-F.** Effects of Trace C Addition on the Microstructure and Refining Efficiency of Al–Ti–B Master Alloy *Journal of Alloys Compounds* 503 2010: pp. 286 – 290. http://dx.doi.org/10.1016/j.jallcom.2010.04.251
20. **Wang, B., Wang, J., Geng, X.-Y., He, D.-P.** Changes of Melting Porosity of Foamed Al Alloy in Solidification Processing *Journal of Southeast University* 30 (6) 2000: pp. 57 – 61.
21. **Yang, D.-H., Hur, B.-Y., Yang, S.-R.** Study on Fabrication and Foaming Mechanism of Mg Foam Using $CaCO_3$ as Blowing Agent *Journal of Alloys Compounds* 61 2008: pp. 221 – 227.
22. **Xia, X.-C., Feng, H., Zhang, X., Zhao, W.-M.** The Compressive Properties of Closed-cell Aluminum Foams

with Different Mn Additions *Materials and Design* 51 2013: pp. 797 – 802.

23. **Paul, A., Ramamurty, U.** Strain Rate Sensitivity of a Closed-cell Aluminum Foam *Materials Science & Engineering A* 281 2000: pp. 1 – 7.
24. **Fang, C.-B., Bai, H.-L., Ye, B., Li, H.** The Influence of the Compound Additive Al-Ti-B and Ce Additive on the A356 Grain Size *Motorcycle Technology* 2010: pp. 58 – 60.
25. **Ni, S.-C.** Condition Resulting in Coarse Grain in Cast-rolled Strip and Measures to Avoid It *Light Alloy Processing Technology* 27 (3) 1999: pp. 11 – 13.
26. **Sritharan, T., Li, H.** Influence of Titanium to Boron Ratio on the Ability to Grain Refine Aluminium–silicon Alloys *Journal of Materials Processing Technology* 63 1997: pp. 585 – 589.
27. **Sigworth, G.-K., Guzowski, M.-M.** Grain Refining of Hypoeutectic Al–Si Alloys *Transactions of the American Fisheries Society* 93 1985: pp. 907 – 912.
28. **Spittle, J.-A., Sadli, S.** Effect of Alloy Variables on Grain Refinement of Binary Aluminium Alloys with Al–Ti–B *Materials Science and Technology* 11 1995: pp. 533 – 537. http://dx.doi.org/10.1179/mst.1995.11.6.533
29. **Kori, S.-A., Auradi, V., Murty, B.-S., Chakraborty, M.** Poisoning and Fading Mechanism of Grain Refinement in Al–7Si Alloy *Materials Forum* 29 2005: pp. 387–393.
30. **Greer, A.-L., Bunn, A.-M., Tronche, A., Evans, P.-V., Bristow, D.-J.** Modelling of Inoculation of Metallic Melts: Application to Grain Refinement of Aluminium by Al-Ti-B *Acta Materialia* 48 2000: pp. 2823 – 2835. http://dx.doi.org/10.1016/S1359-6454(00)00094-X
31. **Koza, E., Leonowic, M., Wojciechowski, S., Simancik, F.** Compressive Strength of Aluminum Foams *Materials Letters* 58 2004: pp. 132 – 135.
32. **Beals, J.-T., Thompson, M.-S.** Density Gradient Effects on Aluminum Foam Compression Behavior *Journal of Materials Science* 32 1997: pp. 3595 – 3600.
33. **Mukai, T., Kanahashi, H., Miyoshi, T., Mabuchi, M., Nieh, T.-G., Higashi, K.** Experimental Study of Energy Absorption in A Close-celled Aluminum Foam under Dynamic Loading *Scripta Materialia* 40 1999: pp. 921 – 927. http://dx.doi.org/10.1016/S1359-6462(99)00038-X
34. **Xia, X.-C., Zhao, W.-M., Feng, X.-Z., Feng, H., Zhang, X.** Effect of Homogenizing Heat Treatment on the Compressive Properties of Closed-cell Mg Alloy Foams *Materials and Design* 49 2013: pp. 19 – 24.
35. **Orbulov, I.-N.** Compressive Properties of Aluminum Matrix Syntactic Foams *Materials Science & Engineering A* 555 2012: pp. 52 – 56.
36. **Zhu, H.-L., Guo, J.-J., Jia, J., Li, P.-Y.** Precipitated Phases of A357 Al Alloy Refined with Ti *Acta Metallurgica Sinica* 36 (1) 2000: pp. 17 – 20.
37. **Lu, L., Lai, M.-O., Chen, F.-L.** Al-4 wt% Cu Composite Reinforced with In-situ TiB2 Particles *Acta Materialia* 45 1997: pp. 4297 – 4309. http://dx.doi.org/10.1016/S1359-6454(97)00075-X
38. **Lee, J., Jung, J.-Y., Lee, E.-S., Park, W.-J., Ahn, S., Kim, N.-J.** Microstructure and Properties of Titanium Boride Dispersed Cu Alloys Fabricated by Spray Forming *Materials Science and Engineering A* 277 2000: pp. 274 – 283.